COMBINED FINANCIAL AND ENVIRONMENTAL OPTIMIZATION OF A TRIGENERATION SYSTEM

*Heber Cláudius Nunes SILVA[1,3], Eric Monroe HORNSBY[3], Filipi Maciel MELO [2,3], Fabio Santana MAGNANI[3], Monica CARVALHO[4], Alvaro Antonio Villa OCHOA[*1,3]*

[1] Federal Institute of Technology of Pernambuco

[2] Federal Institute of Technology of Maranhão

[3] Federal University of Pernambuco

[4] Federal University of Paraiba

[*]ochoaalvaro@recife.ifpe.edu.br, alvaro.ochoa@ufpe.br

Abstract

This paper firstly studies the influence of variations in fuel tariffs and greenhouse gas emissions of the grid electricity on the financial and environmental metrics, demonstrating divergences when considered alone. Secondly, a combined economic and environmental objective function is proposed, yielding a good compromise between both concerns. Real data are available from a Brazilian Northeast building where electricity, heat (hot water), and cooling are important for comfort and well-being. When addressing the bicriteria optimization, consideration of 20% of one metric enormously improved the overall result, with only slightly worsening the other metric. This is possible because the optimization scheme can choose from a rich pool of physical and operational scenarios.

Keywords*: combined cooling heat and power; greenhouse gases; economics; sustainable production; net present value.*

1. Introduction

Trigeneration systems are equipment arrangements responsible for the supply of three energy services, which could be heat, cooling, and electricity. The choice of equipment and the system's topology depends on the hourly variation of demands, tariffs, and technical characteristics. Above all, the topology depends on the purpose of the optimization, which can be the maximization of profit or minimization of environmental emissions. The issue is that financial and environmental metrics seem to be irreconcilable. Electricity consumption in buildings of tropical locations can lead to high economic costs due to air conditioning needs [1]. The high humidity and temperature levels can be challenging when focusing on thermal comfort. Combined cooling, heat, and power energy systems can be a sustainable and reliable way to supply energy to different consumer centers [2]. The most common energy sources in urban areas are fossil fuel lines and public electricity distribution grids, but decentralized renewable energy resources can also be available, such as wind and solar [3], and biomass [4]–[6]. The choice of equipment and the operational settings strongly depend on the daily/seasonal patterns of energy, capital costs of equipment, energy tariffs and technical characteristics of the equipment [7]. Nevertheless, the final topology of an energy system depends primarily on the purpose of the optimization problem. It is common to use the First and Second Laws of thermodynamics to analyze the technical behavior and financial viability of systems aiming to meet the energy demands in different areas, such as: the food industry [7], sugar factory [8], [9], public buildings [10], and the textile industry [11].

Within Linear Programming (LP) problems, Mixed Integer Linear Programming (MILP) has been successfully used to optimize combined energy systems [12], as it shown in Urbanucci [13] where a critical discussion about the advantages and drawbacks of using MILP for optimization was presented, and also, Algieri et al. [14] proposing a novel MILP optimization model for an energy system where the primary energy savings and overall efficiency enhanced by integrating conventional and renewable energy sources. Regarding Brazilian optimization studies, thermoeconomic optimization defined the best waste heat recovery scheme by using ORC as a part of the systems.

From the scientific literature review carried out, it has been demonstrated that several works have developed energy, financial and environmental analyses [2]. Some existing studies even aimed at optimizing trigeneration plants, using methods such as linear programming, and taking technical and economic parameters into account to verify the system's viability [7]. However, there is a clear need to develop and demonstrate a tool capable of assisting in the decision-making of trigeneration system projects, considering aspects such as location, energy and socio-economic policies, and the country's energy matrix. This has not yet been discussed with real applications and results. Therefore, this study proposes an optimization tool that combines financial and environmental aspects to guarantee technical-economic feasibility. It is important to emphasize the lack of studies on this subject, especially considering actual consumption data. The main innovation of this work is the optimization model that is scalable and adaptable to scale and finds the best way to operate trigeneration systems. This study contributes by providing critical results to improve the generation of electricity, heat, and cooling for buildings, considering financial and environmental aspects.

2. Modeling and Optimization for the Trigeneration System

2.1. Description of the Trigeneration System

The combined energy system proposed herein meets the electricity, cooling and heating demands of an office building located in the Brazilian Northeast. Connections are available to the natural gas fuel line and electrical grid. The pieces of equipment available are: a power generator, three boilers (electric, natural gas, and heat recovery), and two chillers (compression and absorption), as depicted in Fig. 1a. EP is the electrical distributor. The electric grid (EG) can meet the electricity demand (ED) directly, or indirectly satisfy the heating and cooling demands, through the electric boiler (EB) and compression chiller (CC), respectively. The fuel line (FL) is connected to the power generator (PG), which can generate electricity. The exhaust gases of PG are harnessed by the heat recovery boiler (RB) to generate steam. There is a steam manifold to combine the shares of steam produced by RB, EB, and the gas boiler (GB), also connected to FL. The steam manifold can meet the heating demand (HD) and supply the absorption chiller (AC). AC and CC supply the building with cooling (CD). There are five types of lines: Fuel (F), Steam (S), Cold Water (CW), Exhaust Gas (EG) and Electricity (E). Each one is indicated in the Fig. 1a by the initial letter and there is also a number indicative which was used in the simulations.

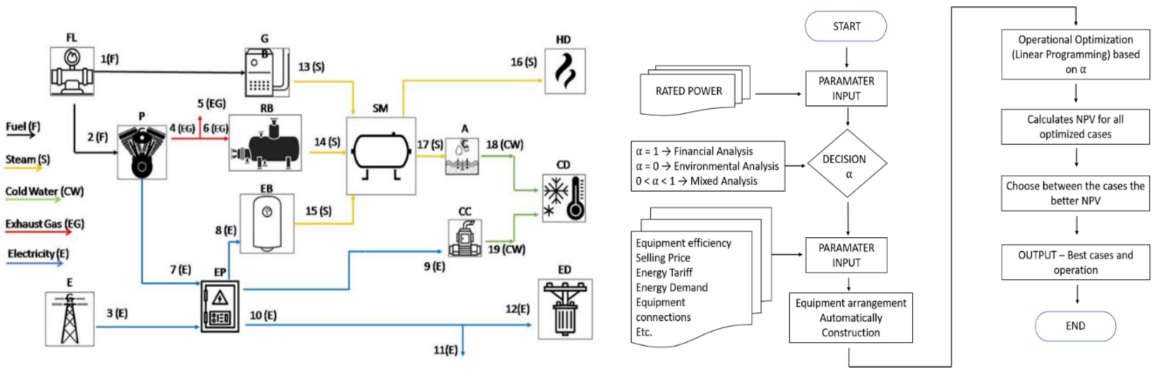

Fig. 1a: Generic floor of the building. **Fig. 1b: Flowchart of the numerical procedure.**

Figure 1. Generic floor and flowchart of the numerical procedure

Real data of equipment and energy demands of a building located in the Brazilian northeast were used; that is, this model is valid for real situations of energy generation and can be applied to other cases, provided that the model developed is well fed with the correct information. All the data used in the simulation are available in tables from 1 to 5 and equations from 1 to 6. This model is an adaptable system. At the beginning of the simulations, it is possible to choose the objective function, that is, whether the cost or emission of pollutants will be optimized. Thus, the percentage of use of each piece of equipment will depend on each simulation, the type of demand, and energy and fuel prices.

2.2. Optimization Problem

2.2.1. Governing Equations

The equations that govern the optimization problem are the objective function (which takes into account financial and environmental indices) and the restriction equations.

The objective function to be maximized (NPV_{comb}, Equation (1)), combines financial (NPV_{fin}) and environmental (NPV_{env}) indices and a financial-environmental factor, α_{FEF}. When α_{FEF} = 1 a financial optimization is carried out, while α_{FEF} = 0 indicates an environmental optimization. Intermediate α_{FEF} values are used for the combined optimization.

$$maximize \quad NPV_{comb} = \alpha_{FEF} NPV_{fin} + (1-\alpha_{FEF}) NPV_{env} \tag{1}$$

The optimization problem contains six discrete and not evenly spaced variables (the rated power of the main equipment, N_i, as seen in Equation 6.), 2736 continuous variables (referring to the 19 energy arrows in Fig.1a, n_{lines}; throughout 144 different hours, n_t), subjected to 2880 restrictions (20 restrictions for each hour).

Equation (2) shows the Financial Net Present Value.

$$NPV_{fin} = -\sum_{i=1}^{N_{eq}} k_{fin,bd,i} N_i + \mu_{fin} \sum_{t=1}^{n_t} \tau_t \{ -k_{fin,fuel}(x_{1,t} + x_{2,t}) - [h_t k_{fin,el,high} + (1 - h_t) k_{fin,el,low}] x_{3,t} + [h_t k_{fin,el,high} + (1-h_t) k_{fin,el,low}] x_{11,t} + [h_t k_{fin,el,high} + (1-h_t) k_{fin,el,low}] x_{12,t} + k_{fin,st,int} x_{16,t} + k_{fin,cw,int}(x_{18,t} + x_{19,t}) \}$$
(2)

In Equation (2), the first term is the total cost of building the system, obtained by multiplying the coefficients representing the specific investment cost, $k_{fin,bd,i}$ [$/kW] by the rated power of each equipment, N_i [kW] (From Fig. 1a: PG, GB, RB, EB, AC, CC). Table 1 shows the specific investment cost for each piece of equipment [15]–[17]. The second term of Equation 2 is the operational value of the system, which accounts for the costs of the monthly consumption of fuel and electricity (negative terms) and the financial returns for supplying the demands and selling the exceeding electricity produced (positive terms).

Table 1. Specific investment cost coefficient.

Equipment	$k_{fin,bd,i}$[$/kW]	Equipment	$k_{fin,bd,i}$[$/kW]
Power Generator (PG)	500	Electric Boiler (EB)	90
Gas Boiler (GB)	90	Absorption Chiller (AC)	516
Recovery Boiler (RB)	200	Compression Chiller (CC)	400

The coefficient $k_{fin,fuel}$ is the fuel tariff, $k_{fin,el,high}$ the on-peak electricity tariff, $k_{fin,el,low}$ is the off-peak electricity tariff. The two last coefficients, $k_{fin,st,int}$, and $k_{fin,cw,int}$, are the tariffs for "selling" the internal energy flows, respectively, in the form of steam and chilled water. The electricity tariff is given by the local concessionaire and the tariffs of steam and chilled water are considered as the cost of production of these utilities by conventional equipment, Table 2 [18]–[20].

Table 2. Energy tariffs.

Coefficient	Value [$/kWh]	Coefficient	Value [$/kWh]
$k_{fin,fuel}$	$1.66\text{x}10^{-8}$	$k_{fin,el,sell,low}$	0.06
$k_{fin,el,high}$	0.13	$k_{fin,st,int}$	0.20
$k_{fin,el,low}$	0.06	$k_{fin,cw,int}$	0.20
$k_{fin,el,sell,high}$	0.13		

In Equation (2), the vector h_t is 1 for the high demand period and = 0 during the low demand period, and the vector τ_t indicates the number of monthly hours represented by time period *t*. For example, if the day is divided in 24 time periods, and if a certain time t represents a period in a weekday, thus τ_t = 21 (21 weekdays periods of one such hour in a month). The term μ_{fin} represents the correction of the number of months, known as the present value factor. The correction is necessary due to the market interest rate (σ) along the total life time of the project (m_t months), as shown in Equation (3).

$$\mu_{fin} = \frac{(1+\sigma)^{m_t}-1}{\sigma(1+\sigma)^{m_t}} \tag{3}$$

The Environmental Net Present Value (NPV_{env}), presented in Equation (4), has a similar mathematical form as NPV_{fin}.

$$NPV_{env} = -\sum_{i=1}^{N_{eq}} k_{env,bd,i} N_i + \mu_{env} \sum_{t=1}^{n_t} \tau_t \{-k_{env,fuel}(x_{1,t} + x_{2,t}) - [h_t k_{env,el,high} + (1 - h_t) k_{env,el,low}] x_{3,t}\}\tau_t \tag{4}$$

The first term stands for the GHG emissions associated with equipment (Table 3) and the second terms refers to the operational GHG emissions, throughout the lifetime of the system. These values were obtained from a Life Cycle Assessment carried out within Simapro 9.0.0.49 [21], using the Ecoinvent database version 3.5 [22], and IPCC 2013 GWP 100y methods [23], which quantifies and groups the GHG emissions in a common metric (CO_2-eq) throughout a time horizon of 100 years.

Table 3. GHG emission factors associated with each piece of equipment.

Equipment	$k_{env,bd,i}$[kg CO_2-eq/kW]	Equipment	$k_{env,bd,i}$[kg CO_2-eq/kW]
Power Generator (PG)	24	Electric Boiler (EB)	53
Gas Boiler (GB)	53	Absorption Chiller (AC)	311
Recovery Boiler (RB)	21	Compression Chiller (CC)	20

Regarding natural gas ($k_{env,fuel}$=0.250 kg CO_2-eq/kWh), the process includes the production and distribution network, plus combustion, for a representative Brazilian process. For the grid electricity ($k_{env,el.high}$=0.259 kg CO_2-eq/kWh and $k_{env,el.low}$=0.259 kg CO_2-eq/kWh), the generation mix considers 71.80% hydroelectricity, 16.70% thermoelectric, 8.30% wind, 2.70% nuclear, and 0.50% solar.

In opposition to the financial analysis, where the financial values must be corrected in time by the present value factor, the monthly GHG emission must be multiplied by the number of months of the operation, as follows:

$$\mu_{env} = m_t \qquad (5)$$

The optimization method chooses the values of the six discrete variables, N_i, among the rated powers given in Equation (6a-6f), Table 4. All the 2736 continuous variables are bounded in the positive domain (Equations 7a-7b), as all pieces of equipment have only one physically possible energy direction.

Table 4. Modeling Equations

N_{GB} = {0, 90, 180, 550, 1100, 1600, 2000}	(6.a)	N_{EB} = {0, 70, 140, 500, 950}	(6.d)
N_{PG} = {0, 70, 140, 500, 950}	(6.b)	N_{AC} = {0, 281.4, 527.6}	(6.e)
N_{RB} = {0, 70, 140, 500, 950}	(6.c)	N_{CC} = {0, 281.4, 527.6}	(6.f)
$0 \leq x_{i,t} \leq \infty$	(7.a)	$1<i<n_{lines}$; $1<t<n_t$	(7.b)
$x_{4,t} - \eta_{PG,th} x_{2,t} = 0$ $1<t<n_t$	(8)	$x_{7,t} - \eta_{PG,el} x_{2,t} = 0$ $1<t<n_t$	(9)
$(x_{8,t} + x_{9,t} + x_{10,t}) - \eta_{EP} x_{7,t} - \eta_{EP} x_{3,t} = 0$ $1<t<n_t$	(10)	$x_{16,t} + x_{17,t} - \eta_{SM} x_{13,t} - \eta_{SM} x_{14,t} - \eta_{SM} x_{15,t} = 0$ $1<t<n_t$	(11)
$x_{14,t} - \eta_{RB} x_{6,t} = 0$ $1<t<n_t$	(12)	$x_{15,t} - \eta_{EB} x_{8,t} = 0$ $1<t<n_t$	(13)
$x_{13,t} - \eta_{GB} x_{1,t} = 0$ $1<t<n_t$	(14)	$x_{18,t} - COP_{AC} x_{17,t} = 0$ $1<t<n_t$	(15)
$x_{19,t} - COP_{CC} x_{9,t} = 0$ $1<t<n_t$	(16)	$x_{4,t} - x_{5,t} - x_{6,t} = 0$ $1<t<n_t$	(17)
$x_{10,t} - x_{11,t} - x_{12,t} = 0$ $1<t<n_t$	(18)	$x_{18,t} + x_{19,t} = W_t$ $1<t<n_t$	(19)
$x_{12,t} = E_t$ $1<t<n_t$	(20)	$x_{16,t} = S_t$ $1<t<n_t$	(21)
$N_{PG} - x_{7,t} \geq 0$ $1<t<n_t$	(22)	$N_{GB} - x_{13,t} \geq 0$ $1<t<n_t$	(23)
$N_{RB} - x_{14,t} \geq 0$ $1<t<n_t$	(24)	$N_{EB} - x_{15,t} \geq 0$ $1<t<n_t$	(25)
$N_{AC} - x_{18,t} \geq 0$ $1<t<n_t$	(26)	$N_{CC} - x_{19,t} \geq 0$ $1<t<n_t$	(27)

For each time period, the continuous variables, $x_{i,t}$, are furtherly submitted to 20 restrictions depending on equipment efficiencies (Equations (8 – 16)), energy conservation (Equations (17 -18)), energy demands (Equations (19 – 21)) and rated powers (Equations (22 -27)). Fixed values were employed for the equipment.

The power generator is subjected to Equations (8) and (9), which represent the portion of the fuel's energy transferred to the hot gases (Equation (8)) and the electric power produced by the generator in each time interval (Equation (9)).

The distribution panel that combines the electric power from the grid and the generator is modelled by Equation (10).

Equation (11) represents the energy flows of the steam manifold, taking into account its efficiency, η_{SM}.

The specific efficiencies of the three boilers, Equations (12 – 14), relate inlet and outlet:

The COPs of both chillers, Equations (15 – 16), relates their cooling power with the power consumption.

Equation (17) shows that the exhaust gases produced by the power generator, $x_{4,t}$, are used by the recovery boiler, $x_{6,t}$, or else evacuated to the atmosphere, $x_{5,t}$.

The electricity not used by the compression chiller or the electric boiler can be exported to the electric grid, $x_{11,t}$, or used to meet the demand, $x_{12,t}$, as expressed by Equation 18.

The demand vectors were obtained a priori by Magnani et al. [47], for chilled water (W_t), electricity (E_t) and steam (S_t), and satisfied by Equations (19 – 21).

The last 864 (= 6 equations x 144 different hours, t) inequality restrictions, Equations (22 – 27), restrict the produced power of each piece of equipment to its rated power.

A hybrid method is employed, based on Magnani et al. [24], which consisting of five steps:

Step 1: proposal of the generic system. In this paper, the generic system is presented in Fig. 1a, so the optimal system will always be a subsystem of the generic one.

Step 2: pre-selection of the equipment. Selection of the possible rated powers for each main equipment, as given by Equation (6).

Step 3: permutation. Creation of all the possible permutation of equipment given by Equation (6), in this case 7875 (=7.5.5.5.3.3).

Step 4: linear programming. The choice of specific values for N_i is made through the presented linear programming model, where an objective function is optimized, based on physical and energy constraints. In this paper, we performed 7,875 linear optimizations.

Step 5: choice of the best case. In this step the best NPV_{comb} is selected, among all the optimizations of step #4.

Please note that step #3 is related to the design of the system (definition of its topology), while step #4 relates to its operation. Thus, step #5 integrates both the design and operation optimization of the system. The computational model optimized 5472 energy flow variables from 7875 cases in an approximate time of 16300 seconds.

2.2.2. Financial and Environmental Indices

For each design configuration and operational settings, it is possible to quantify two metrics for the system: the Financial Net Present Value (NPV_{fin}) and the Environmental Net Present Value (NPV_{env}). It is really important to know if the initial monetary investment will be paid off, and the same applies to the embedded emissions within the energy system.

The first part of the algorithm used in this work calculates the initial investment for each scenario. The second part optimizes each operation for each scenario, taking into account the energy demands and costs involved. The calculation of was shown in section 3.1.

Some variables are used to verify the impact of a specific variable on the metric, and this type of analysis is crucial to see what happens if fuel tariffs increase or electricity prices decrease, for example. The prices are not static, and with *NPV* metrics it is possible to see the impact throughout the years.

3. Numerical Proceeding of the Modeling

The process only starts after inserting an input dataset and choosing the α factor to weight the financial and environmental objectives, as show in Fig. 1b. After all possible cases are generated, the linear programming model starts to optimize the operation of all cases by maximizing the objective function, respecting the constraints of the optimization problem. The option with the highest objective function value is selected, resulting in two decision variables: the best topology (configuration) and its best operation.

4. Results and Discussion

The objective of this work was to show that the model developed works and meets the need for dimensioning and optimization of operation in a dynamic way, where it would be possible to know how the system will operate in the period determined at the beginning of the simulation. The next phase would be to determine the most critical factors in the choice of equipment and forms of operation through sensitivity analysis, bringing more critical information for the decision-making of whoever uses the developed model. One of the concerns of our work is the performance of the chillers, in this case, the absorption chiller. Chiller load is a concern for the deployed system. However, it was only observed the total chiller load. Hence, it was considered three case studies. The first verify the influence of the fuel tariff on the maximal financial objective, NPV_{fin} (α_{FEF}=1). Then the influence of GHG emissions from the electric grid is verified by optimizing the system for a minimum absolute value of environmental NPV_{env} (α_{FEF}=0). Finally, the influence of the financial-environmental factor (α_{FEF}) is tested by optimizing the energy system with NPV_{comb}.

4.1. Influence of the Fuel Tariff on the Optimal Financial Systems

The general layout illustrated by Fig. 2 is used to present the results. The x-axis refers to the factor being varied, in this case the percentage increase or decrease (β_{fuel}) of the fuel tariff. The right y-axis is the NPV_{fin}, in this case the primary optimized curve, presented by a continuous line, and the left y-axis is NPV_{env}, the secondary measured value, presented by a dotted line. In Fig. 2, it can be observed that when the fuel tariff is near zero the system is quite profitable as it is exporting the maximum amount of surplus electricity. On the other hand, *NPVenv* is too low because of fossil fuel is used to feed the equipment that are working to attend the energy demand. Also, can be seen in Fig. 2, a point where those two lines intersect. At this point, there is a balance between the two metrics studied. In works like Gao et al. [25] and Dabwan and Pei [26], those two metrics are studied separately and it is hard to connect the relationship between these two variables, and also in Melo et al. [27], it was possible to find solutions that had a huge environmental commitment with small financial losses.

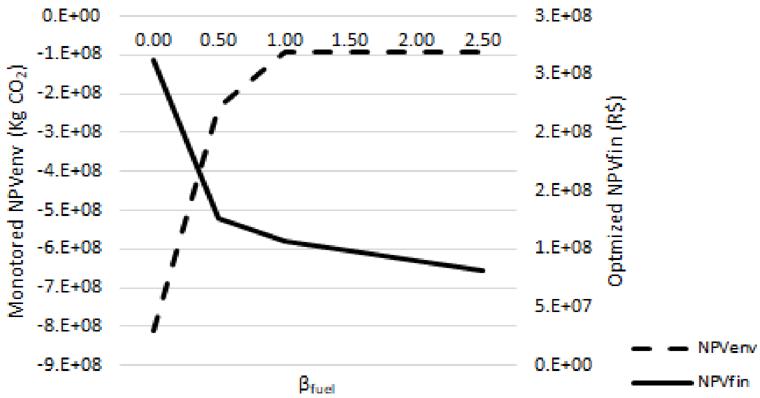

Fig. 2. Influence of the fuel tariff on the optimal systems considering NPV_{fin} (α_{FEF}=1).

Fig. 3 presents the electrical operation of the system with β_{fuel} = 0 for a representative day. (a) represents the input of electricity into the system and (b) represents the output of electricity. It is observed that all electricity input comes from the power generator in X7 (power in energy flow number 7 in Fig. 1) and the largest amount of this electricity will be sold in X20 (power in energy flow number 20 in Fig. 1).

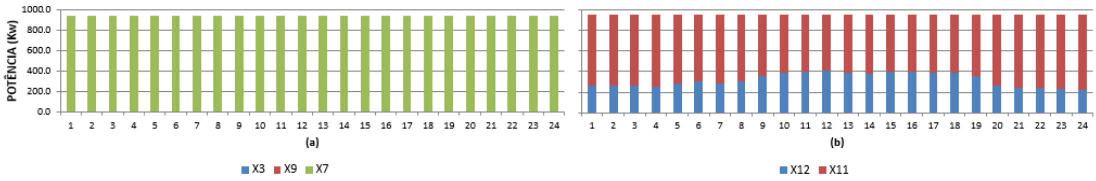

Fig. 3. electrical operation of the system. (a) represents the input of electricity into the system and (b) represents the output of electricity

The profitability drops sharply as the fuel price increases. Table 4 indicates which equipment is chosen in each β_{fuel} range regarding the optimization of the financial net present value (NPV_{fin}).

Table 4. Physical configurations for the optimal financial systems when the fuel tariff varies (β_{fuel}).

β_{fuel}		Rated Power [kW]					
Lower	Upper	N_{PG}	N_{GB}	N_{RB}	N_{EB}	N_{AC}	N_{CC}
0.0	0.49	950	1100	140	0	527	0
0.5	0.99	950	0	950	0	281	281
1.0	2.5	0	550	0	0	0	527

From the analysis of Fig. 3, Fig. 4 and Table 4, as the price of fuel increases and the system starts to rely more on electrical equipment, there is a decrease in GHG emissions. This occurs because the Brazilian electricity mix is comprised mostly of hydroelectricity, with low associated GHG emissions. The great variation in the equipment selected in the optimization process highlights the importance of including all possible energy conversion technologies, other works, such as Mohammadi et al. [29], and also Melo et al. [30] emphasizes this.

4.2. Influence of the GHG Emissions from the Electricity Grid on the Optimal Environmental Systems

Fig. 4a shows the results of the environmental optimization, varying the GHG emissions of the electric grid (base value multiplied by β_{emis}). As the GHG emissions of the grid vary, the dotted line shows the optimized NPV_{env} (GHG released) and the solid line indicates the monitored NPV_{fin}. β_{emis} =1 represents a grid based majorly on hydroelectricity. The curve indicates that as the GHG emissions of the grid increase, the less profitable the system becomes. Table 5 indicates which equipment is chosen for each β_{emis} range.

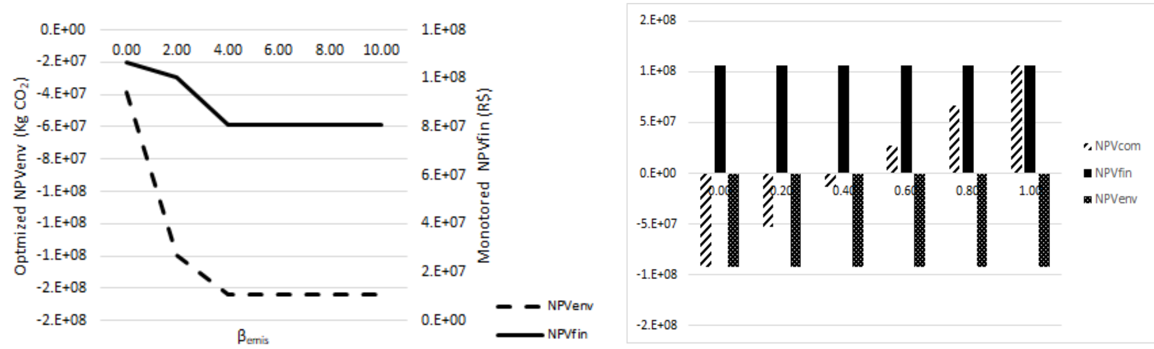

4 (a) **4 (b)**

Fig. 4a. Influence of the GHG emissions of the electric grid on the optimal environmental systems NPV_{env} (α_{FEF}=0). 4b. Influence of the financial-environmental factor (α_{FEF}) on systems optimized for the combined metric NPV_{comb} (base case, β_{fuel}=β_{emis}=1).

The profitability drops sharply as the fuel price increases. Table 4 indicates which equipment is chosen in each β_{fuel} range regarding the optimization of the financial net present value (NPV_{fin}). Table 5 indicates that as the GHG emissions associated with the electric grid increase, the optimal system will rely less on electrical equipment, increasing the operation costs of the system.

Table 5. Physical configurations for the optimal environmental systems when β_{emis} varies.

β_{emis}		Rated Power [kW]					
Lower	Upper	N_{PG}	N_{GB}	N_{RB}	N_{EB}	N_{AC}	N_{CC}
0.0	1.9	0	550	0	0	0	527
2.0	3.9	500	550	500	0	0	527
4.0	10.0	950	550	950	0	281	527

4.3. Influence of the Financial-Environmental Factor (α_{FEF}) on the Optimal Systems Optimized by the Combined Metric NPV_{comb}

It is necessary to choose well which parameter will be used to optimize the results, as can be seen in Melo et al. [27]. This topic analyzes the influence of the choice of the factor that defines whether the analysis will be environmental, financial or partial, in a combined *NPV*. Fig. 4a shows the effect of α_{FEF} on the optimal systems. In Fig. 4b, when α_{FEF} = 0 and α_{FEF} = 1 there is the same amount of GHG emissions and financial values. This happens because the system does not change with α_{FEF}. In other words, a change in α_{FEF} did not result in an adaptation of the configuration or operation of the system, demonstrating the resilience of the system. Table 6 shows the system for all α_{FEF} values and their respective NPV_{fin} and NPV_{env} value.

Table 6. Physical configurations for the optimized systems with financial-environmental factor (α_{FEF}). Rated powers in kW, net present values in millions of US$/kg of CO_2-eq.

α_{FEF}	N_{PG}	N_{GB}	N_{RB}	N_{EB}	N_{AC}	N_{CC}	NPV_{fin}	NPV_{env}
0 - 1	0	550	0	0	0	527.6	1.1E8	-9.2E7

Hou et al. [31] evaluated a conventional Combined Cooling, Heat and Power (CCHP) system and a hybrid energy distributed generation system, proposing a new operation strategy in the optimization process. Their results indicated that the conventional CCHP system could reduce 15.2% of CO_2 emissions when compared to an operation strategy following the thermal load (FLT - widely used in non-linear optimization processes).

The results of section 4.1 show that, as the fuel tariff increases, the system becomes less polluting, replacing fuel-consuming equipment with equipment that consumes electricity from the grid, with low GHG emissions. As a result, the system is less profitable as there is no monetization associated with the reduction of GHG emissions in the model. It could be possible to obtain environmental and financial advantages with CCHP systems if legal aspects take into account a financial benefit related to a reduction in GHG emissions. The optimization of CCHP systems is site-dependent and directly related input data, such as hourly-seasonal energy demands and equipment parameters (technical, financial and environmental). Local regulations can affect the connection to the electric grid, but there is also a strong influence of local energy tariffs and climate data. In this context, Ren et al. [32] proposed multi-objective optimization to study different types of buildings in China, considering financial and environmental aspects. The results indicated that the configuration and operation of the systems are closely related to the type of building considered.

Section 4.2 focused on the GHG emissions associated with the electric grid. It was observed that any investments directed to maintain a low-carbon electric mix are financially worthwhile as this also reduces the capital costs of the CCHP. In Brazil, the electricity mix is predominantly renewable, consisting mainly of hydroelectricity. However, when water crises occur, fossil fuels are employed to meet energy demands, obviously increasing the GHG emissions of the electric grid. According to the Atlas of Brazilian Wind Potential [33] hydroelectricity and wind electricity are complementary. The addition of wind energy to the electric mix promotes enhanced seasonal stability in the supply of low-carbon electricity in Brazil [34], [35].

Section 4.3 showed that the solution of the linear programming problem yielded a conventional system, consisting of a vapor compression chiller that met the cooling demand, a gas boiler that met the demand of heat, and the electricity demand was met directly by the electric grid. Although the model enables several optimal solutions, the method found a global solution, resilient to the α_{FEF} change, which weighs the financial and environmental objective.

National incentive policies could be formulated to incentivize and prioritize high-efficiency solutions. Espirito Santo et al. [36] suggested using the metric of primary energy savings (PES) to compare combined energy systems with conventional, centralized thermal plants. The authors also suggest that Brazil could establish an energy program to increase the efficiency of centralized thermal plants and use this target to define combined energy scheme incentives. A threshold value of PES could be formulated and incorporated within optimization problems.

Finally, the consideration of combined energy systems is very important to support the energy transition, and this cascading use of energy has proven benefits from financial and environmental viewpoints. However, the adoption of combined energy systems has been undoubtedly underexplored as it was described in Marques et al. [37], especially in Brazil. As mentioned, combined energy systems can and must be part of energy efficiency solutions to enhance economic competitiveness, providing more affordable energy services, and reducing environmental impacts.

5. Conclusion

The optimal global solution consisted of a conventional system, constituted by a gas boiler and compression chiller to meet the heat and cooling demands, respectively, while the electricity demand was met directly by purchasing electricity from the grid. It was observed that as the fuel tariff increases, the system becomes less financially profitable and less polluting. This occurs because the solution of the optimization problem replaces natural gas-equipment with electrical equipment, and relies more on the electricity grid, which is predominantly renewable in Brazil. When evaluating the variation in the GHG emissions associated with the electricity grid, an increase in grid emissions results in lower economic benefits. Investments in low-carbon energy generation schemes should be incentivized, as herein economic benefits were realized (with decreases in the capital costs of the energy system).

Acknowledgments

The authors would like to thank the Graduate Program in mechanical Engineering from the Federal University of Pernambuco (PPGEM/UFPE) for its support within the PhD program. The fourth and fifth authors thank the Brazilian National Council for Scientific and Technological Development (CNPq) for their Research Productivity grants nº 307394/2018-2 and 309154/2019-7.

Nomenclature

AC - absorption chiller
CC - compression chiller
CCHP - combined cooling heat and power
EB – electric boiler
ED - electricity demand
EG - electric grid
PG - power generator
FL - fuel line
GB - gas boiler
RB - recovery boiler
HD - heat demand
CD - cold water demand

Variables

β_{ele} - variable that multiplies the electricity tariff.
β_{fuel} - variable that multiplies the fuel tariff
COP_{AC} - performance coefficient of the absorption chiller
COP_{CC} - performance coefficient of the compression chiller
σ - interest rate
$K_{env,bd,i}$ - environmental coefficient of the respective equipment i ($kgCO_{2-eq}$/kW)
$K_{env,el,hight}$ - peak hour environmental coefficient ($kgCO_{2-eq}$ /kWh)
$K_{env.el.low}$ – off-peak environmental coefficient ($kgCO_{2-eq}$ /kWh)
$K_{fin,el,hight}$ - peak hour electricity tariff ($/kWh)
$K_{fin.el.low}$ – off-peak electricity tariff ($/kWh)
$K_{fin,fue}l$ - fuel tariff ($/kWh)
$K_{env,fue}l$ - fuel emission tariff ($kgCO_{2-eq}$ /kWh)
$K_{fin,bd,i}$ - investment cost coefficient of the respective equipment i ($/kW)
m_t - lifetime of the system (months)
N_i - power of the respective equipment i (kW)
NPV_{comb} - Net Present Value
NPV_{fin} – Financial Net Present Value
NPV_{env} - Environmental Net Present Value
t - characteristic time interval
$X_{1,t}$ - power on line 1 at characteristic time interval t
$X_{2,t}$ - power on line 2 at characteristic time interval t
$X_{3,t}$ - power on line 3 at characteristic time interval t
$X_{4,t}$ - power on line 4 at characteristic time interval t
$X_{5,t}$ - power on line 5 at characteristic time interval t
$X_{6,t}$ - power on line 6 at characteristic time interval t
$X_{7,t}$ - power on line 7 at characteristic time interval t
$X_{8,t}$ - power on line 8 at characteristic time interval t
$X_{9,t}$ - power on line 9 at characteristic time interval t
$X_{10,t}$ - power on line 10 at characteristic time interval t
$X_{11,t}$ - power on line 11 at characteristic time interval t
$X_{12,t}$ - power on line 12 at characteristic time interval t
$X_{13,t}$ - power on line 13 at characteristic time interval t
$X_{14,t}$ - power on line 14 at characteristic time interval t
$X_{15,t}$ - power on line 15 at characteristic time interval t
$X_{16,t}$ - power on line 16 at characteristic time interval t
$X_{17,t}$ - power on line 17 at characteristic time interval t
$X_{18,t}$ - power on line 18 at characteristic time interval t
$X_{19,t}$ - power on line 19 at characteristic time interval t
μ - present value factor.
η_{EB} - efficiency of the electrical boiler
$\eta_{PG,el}$ - electrical efficiency of the engine-generator set
$\eta_{PG,th}$ - thermal efficiency of the engine-generator set
η_{RB} - efficiency of the recovery boiler
η_{GB} - efficiency of the gas boiler

References

[1] N. M. Kumar, M. Samykano, and A. Karthick, “Energy loss analysis of a large scale BIPV system for university buildings in tropical weather conditions: A partial and cumulative performance ratio approach,” *Case Stud. Therm. Eng.*, vol. 25, no. February, p. 100916, 2021, doi: 10.1016/j.csite.2021.100916.

[2] M. V. Mančić, D. S. Živković, M. L. Djordjević, M. S. Jovanović, M. N. Rajić, and D. M. Mitrović, “Techno-economic optimization of configuration and capacity of a polygeneration system for the energy demands of a public swimming pool building,” *Therm. Sci.*, vol. 22, pp. S1535–S1549, 2018, doi: 10.2298/TSCI18S5535M.

[3] F. Weschenfelder *et al.*, “A review on the complementarity between grid-connected solar and wind power systems,” *J. Clean. Prod.*, vol. 257, p. 120617, 2020, doi: 10.1016/j.jclepro.2020.120617.

[4] H. Topal, T. Taner, Y. Altinsoy, and E. Amirabedin, “Application of trigeneration with direct co-combustion of poultry waste and coal a case study in the poultry industry from Turkey,” *Therm. Sci.*, vol. 22, no. 6, pp. 3073–3082, 2018, doi: 10.2298/TSCI170210137T.

[5] T. Taner and M. Sivrioglu, “A techno-economic & cost analysis of a turbine power plant: A case study for sugar plant,” *Renew. Sustain. Energy Rev.*, vol. 78, no. May, pp. 722–730, 2017, doi: 10.1016/j.rser.2017.04.104.

[6] T. Taner, “Optimisation processes of energy efficiency for a drying plant: A case of study for Turkey,” *Appl. Therm. Eng.*, vol. 80, pp. 247–260, 2015, doi: 10.1016/j.applthermaleng.2015.01.076.

[7] S. C. S. Alcântara, A. A. V. Ochoa, J. A. P. da Costa, P. S. A. Michima, and H. C. N. Silva, “Natural gas based trigeneration system proposal to an ice cream factory: An energetic and economic assessment,” *Energy Convers. Manag.*, vol. 197, no. April, p. 111860, 2019, doi: 10.1016/j.enconman.2019.111860.

[8] T. Taner and M. Sivrioglu, “Energy-exergy analysis and optimisation of a model sugar factory in Turkey,” *Energy*, vol. 93, pp. 641–654, 2015, doi: 10.1016/j.energy.2015.09.007.

[9] T. Taner, M. Sivrioğlu, H. Topal, A. S. Dalkılıç, and S. Wongwises, “A model of energy management analysis, case study of a sugar factory in Turkey,” *Sadhana - Acad. Proc. Eng. Sci.*, vol. 43, no. 3, 2018, doi: 10.1007/s12046-018-0793-2.

[10] H. C. N. Silva, J. C. C. Dutra, J. A. P. Costa, A. A. V. Ochoa, C. A. C. dos Santos, and M. M. D. Araújo, “Modeling and simulation of cogeneration systems for buildings on a university campus in Northeast Brazil – A case study,” *Energy Convers. Manag.*, vol. 186, no. September 2018, pp. 334–348, 2019, doi: 10.1016/j.enconman.2019.02.062.

[11] Leite *et al.*, “Natural gas based cogeneration system proposal to a textile industry: a financial assessment,” *Energy Effic.*, vol. 14, no. 2, 2021, doi: 10.1007/s12053-021-09927-2.

[12] B. S. M. C. Borba, L. F. Henrique, and D. C. Malagueta, “A novel stochastic optimization model to design concentrated photovoltaic/thermal systems: A case to meet hotel energy demands compared to conventional photovoltaic system,” *Energy Convers. Manag.*, vol. 224, no. September, p. 113383, 2020, doi: 10.1016/j.enconman.2020.113383.

[13] L. Urbanucci, “Limits and potentials of Mixed Integer Linear Programming methods for optimization of polygeneration energy systems,” *Energy Procedia*, vol. 148, pp. 1199–1205, 2018, doi: 10.1016/j.egypro.2018.08.021.

[14] A. Algieri, P. Beraldi, G. Pagnotta, and I. Spadafora, “The optimal design, synthesis and operation of polygeneration energy systems: Balancing life cycle environmental and economic priorities,” *Energy Convers. Manag.*, vol. 243, no. February, p. 114354, 2021, doi: 10.1016/j.enconman.2021.114354.

[15] X. Luo, J. Liu, Y. Liu, and X. Liu, “Bi-level optimization of design, operation, and subsidies for standalone solar/diesel multi-generation energy systems,” *Sustain. Cities Soc.*, vol. 48, no. December 2018, p. 101592, 2019, doi: 10.1016/j.scs.2019.101592.

[16] L. Li, H. Mu, N. Li, and M. Li, “Economic and environmental optimization for distributed energy resource systems coupled with district energy networks,” *Energy*, vol. 109, pp. 947–960, 2016, doi: 10.1016/j.energy.2016.05.026.

[17] M. De Sousa Teixeira and S. De Oliveira Júnior, “Thermoeconomic evaluation of cogeneration systems for a chemical plant,” *Int. J. Appl. Thermodyn.*, vol. 4, no. 3, pp. 157–163, 2001, doi: 10.5541/ijot.76.

[18] A. Asadi, M. Meratizaman, and A. A. Hosseinjani, “Feasibility study of small-scale gas engine integrated with innovative net-zero water desiccant cooling system and single-effect thermal desalination unit,” *Int. J. Refrig.*, vol. 119, pp. 276–293, 2020, doi: 10.1016/j.ijrefrig.2020.06.025.

[19] COPERGAS, “Tarifas - 2021. [Online]. Available: .,” 2020. https://www.copergas.com.br/atendimento -ao-cliente/tarifas/.

[20] ANEEL, *APPROVAL RESOLUTION No. 2530 OF APRIL 16, 2019*. 2019.

[21] PréConsultants, “Simapro software,” 2019. https://www.simapro.com.

[22] Ecoinvent, “Ecoinvent. Database, version 3.5.,” 2019. http://www.ecoinvent.org.

[23] IPCC, “Intergovernmental Panel on Climate Change. Report Climate Change 2013: The Physical Science Basis.,” NY/USA, 2013.

[24] F. S. Magnani, P. P. da Silva, M. R. Guerra, and E. M. Hornsby, “Adaptability of optimized cogeneration systems to deal with financial changes occurring after the design period,” *Energy Build.*, vol. 58, pp. 183–193, Mar. 2013, doi: 10.1016/j.enbuild.2012.11.023.

[25] Z. Gao, L. Guo, W. Ji, H. Xu, B. An, and J. Wang, “Thermodynamic and economic analysis of a trigeneration system based on liquid air energy storage under different operating modes,” *Energy Convers. Manag.*, vol. 221, no. July, p. 113184, 2020, doi: 10.1016/j.enconman.2020.113184.

[26] Y. N. Dabwan and G. Pei, “A novel integrated solar gas turbine trigeneration system for production of power, heat and cooling: Thermodynamic-economic-environmental analysis,” *Renew. Energy*, vol. 152, pp. 925–941, 2020, doi: 10.1016/j.renene.2020.01.088.

[27] F. M. Melo, F. S. Magnani, and M. Carvalho, “A decision-making method to choose optimal systems considering financial and environmental aspects: Application in hybrid CCHP systems,” *Energy*, vol. 250, p. 123816, 2022, doi: 10.1016/j.energy.2022.123816.

[28] F. Calise, F. L. Cappiello, M. Dentice d’Accadia, and M. Vicidomini, “Thermo-economic optimization of a novel hybrid renewable trigeneration plant,” *Renew. Energy*, vol. 175, pp. 532–549, 2021, doi: 10.1016/j.renene.2021.04.069.

[29] K. Mohammadi, M. S. E. Khaledi, M. Saghafifar, and K. Powell, “Hybrid systems based on gas turbine combined cycle for trigeneration of power, cooling, and freshwater: A comparative techno-economic assessment,” *Sustain. Energy Technol. Assessments*, vol. 37, no. December 2019, 2020, doi: 10.1016/j.seta.2020.100632.

[30] F. M. Melo,, F. S. Magnani, and M. Carvalho, “optimization of an integrated combined cooling, heat, and power system with solar and wind contribution for buildings located in tropical areas,” *Int. J. energy reserach*, vol. 46, no. 1, pp. 1263–1284, 2021, doi: 10.1002/er.7244.

[31] J. Hou, J. Wang, Y. Zhou, and X. Lu, “Distributed energy systems: Multi-objective optimization and evaluation under different operational strategies,” *J. Clean. Prod.*, vol. 280, p. 124050, 2021, doi: 10.1016/j.jclepro.2020.124050.

[32] F. Ren, Z. Wei, and X. Zhai, “Multi-objective optimization and evaluation of hybrid CCHP systems for different building types,” *Energy*, vol. 215, p. 119096, 2021, doi: 10.1016/j.energy.2020.119096.

[33] O. A. C. . Amarante, M. . Brower, J. . Zack, and A. L. de Sá, *Atlas do Potencial Eólico Brasileiro*. 2001.

[34] J. Schmidt, R. Cancella, and A. O. Pereira, “An optimal mix of solar PV, wind and hydro power for a low-carbon electricity supply in Brazil,” *Renew. Energy*, vol. 85, no. 2016, pp. 137–147, 2016, doi: 10.1016/j.renene.2015.06.010.

[35] C. Viviescas *et al.*, “Contribution of Variable Renewable Energy to increase energy security in Latin America: Complementarity and climate change impacts on wind and solar resources,” *Renew. Sustain. Energy Rev.*, vol. 113, no. November 2017, 2019, doi: 10.1016/j.rser.2019.06.039.

[36] D. B. do Espirito Santo and W. L. R. Gallo, “Utilizing primary energy savings and exergy destruction to compare centralized thermal plants and cogeneration/trigeneration systems,” *Energy*, vol. 120, no. december 2006, pp. 785–795, 2017, doi: 10.1016/j.energy.2016.11.130.

[37] A. S. Marques, M. Carvalho, A. A. V. Ochoa, R. Abrahão, and C. A. C. Santos, “Life cycle assessment and comparative exergoenvironmental evaluation of a micro-trigeneration system,” *Energy*, vol. 216, no. xxxx, 2021, doi: 10.1016/j.energy.2020.119310.

Paper submitted: 04.08.2022
Paper revised: 22.09.2022
Paper accepted: 30.09.2022